SERS uncovers the link between conformation of cytochrome *c* heme and mitochondrial membrane potential

Nadezda A. Brazhe[1§*], Evelina I. Nikelshparg[1§], Adil A. Baizhumanov[1], Vera G. Grivennikova[2], Anna A. Semenova[3], Sergey M. Novikov[4], Valentyn S. Volkov[4,5], Aleksey V Arsenin[4], Dmitry I. Yakubovsky[4], Andrey B. Evlyukhin[4,6], Zhanna V. Bochkova[1], Eugene A. Goodilin[3,7,8], Georgy V. Maksimov[1,9], Olga Sosnovtseva[10#*], Andrey B. Rubin[1#]

[1] Department of Biophysics, Biological Faculty, Moscow State University, Russia

[2] Department of Biochemistry, Biological Faculty, Moscow State University, Russia

[3] Faculty of Materials Sciences, Moscow State University, Russia

[4] Center for Photonics and 2D Materials, Moscow Institute of Physics and Technology, Russia

[5] GrapheneTek, Skolkovo Innovation Center, Moscow, Russia

[6] Institute of Quantum Optics, Leibniz Universität Hannover, Hannover, Germany

[7] Faculty of Chemistry, Moscow State University, Russia

[8] Kurnakov Institute of General and Inorganic Chemistry RAS, Moscow, Russia

[9] Federal State Autonomous Educational Institution of Higher Education “National Research Technological University “MISiS”, Moscow, Russia

[10] Department of Biomedical Sciences, Faculty of Health and Medical Sciences, University of Copenhagen, Denmark

[§]equal contribution

[#] shared co-supervision

*Corresponding author's email: nadezda.brazhe@biophys.msu.ru; olga@sund.ku.dk

Abstract

Cytochrome *c* is an essential component of the electron transport chain (ETC), which regulates respiratory chain activity, oxygen consumption, and ATP synthesis. But the impact of conformational changes in cytochrome *c* on its function is not understood for lack of access to these changes in intact mitochondria. Here we describe a label-free tool that identifies conformational changes in cytochrome *c* heme and elucidates their function. We verify that molecule bond vibrations assessed by surface-enhanced Raman spectroscopy (SERS) is a reliable indicator of the planar heme configuration during activation of ETC and decrease in inner mitochondrial membrane potential. The planar conformation of cytochrome *c* heme enables its optimal orientation towards the heme of cytochrome *c1* in complex III. This ensures a faster electron transfer, which is important during ETC speed-ups and acceleration of ATP synthesis. The ability of our tool to track mitochondrial function opens wide perspectives on cell bioenergetics.

Introduction

Mitochondrial respiratory chain (electron transport chain, ETC) provides oxidative phosphorylation (OXPHOS) and plays a crucial role in the production of reactive oxygen species (ROS), initiation of apoptosis, maintenance of Ca^{2+} concentration in cytoplasm and its storage[1,2,3]. ETC activity determines the efficiency of ATP synthesis. An imbalance between ETC activity and the amount of ATP needed by the cell may lead to ATP deficiency and suppression of the cell function or to the excessed ROS production in ETC, oxidative stress, and cytochrome *c*-dependent apoptosis[4,5,6,7]. To eliminate these negative effects mitochondria possess various regulatory mechanisms to adjust the activity of ETC complexes to the optimal rate of ATP synthesis. Numerous studies on ETC complexes I, III and IV demonstrated high importance of their local conformation, interaction with membrane lipids and with one another for the formation of supramolecular complex of respirasome[4], for the optimization of the electron transport, and for the minimization of ROS production[8,9].

Cytochrome *c* (cytC) is the only soluble electron carrier in ETC, transferring electrons from *bc1*-complex (complex III) to cytochrome *c* oxidase (complex IV) by means of diffusion in the mitochondrial intermembrane space (IMS)[10]. CytC is also involved into ROS formation and scavenging; it can initiate apoptosis by leaving mitochondria[5, 10, 11]. CytC is a small globular protein containing heme *c* (iron porphyrin cofactor) that is covalently bound to the protein chain via two Cys-side radicals and has four tissue-specific phosphorylation[12,13,14,15]. Phosphorylation of cytC affects its activity and the whole OXPHOS. This was demonstrated for mitochondria in heart, brain, liver, skeletal muscles, and kidney[12,13,14,15]. Huttemann et al. suggested that high membrane potentials ($\Delta\Psi$) drive cytC phosphorylation in order to prevent IMM hyperpolarization and ROS production: in cardiomyocytes under high $\Delta\Psi$ cytC is phosphorylated on Tyr97 residue leading to a decrease in $\Delta\Psi$ and ROS production[12]. It was also revealed that the heme iron-Met80 absorption band (695 nm) is down-shifted under Tyr97 phosphorylation, suggesting the existence of

phosphorylation-evoked conformational changes in heme[16]. Since the conformation of cytC heme is essential for its orientation towards heme *c1* in complex III or Cu A center in complex IV, the modified heme conformation in phosphorylated cytC can contribute to the changes in ETC activity. Growing evidence indicates that cytC activity can be regulated not only by the modification of the cytC protein part but also by heme conformational changes. It is known that cytC heme predominantly exists in two conformations: planar and ruffled[17]. The probability for planar and ruffled heme conformations differs for purified wild type cytC and its various mutant forms; cytC mutants with the ruffled heme have a decreased rate of electron transfer between cytC – complex III and cytC – complex IV[17,18]. Experiments on the solution of purified oxidized cytC under high electric fields also revealed ruffled heme conformation[19]. In mitochondria, there is also a possibility that the inner mitochondrial membrane potential ($\Delta\Psi$) can change heme conformation affecting cytC ability to accept or donate an electron.

Despite numerous studies on isolated cytC there is a lack of understanding of cytC conformational and dynamical changes as well as cytC tuning mechanisms to comply with electron flux in ETC in living mitochondria. To assess if cytC molecules can switch between planar and ruffled heme conformations and which factors can cause this it is crucial to perform non-invasive label-free studies under modulation of the electron transport. Raman spectroscopy (RS) was used to study reduced *c*- and *b*-type cytochromes in isolated cytochromes and ETC complexes, cells, tissues, and whole organs[20,21,22,23,24,25]. However, RS can not clearly distinguish between reduced *c*- and *b*-types of cytochromes, and can not provide information about certain heme conformations. Oxidized cytochromes in ETC of mitochondria remain undetected because of their weak Raman scattering. We successfully applied surface-enhanced Raman spectroscopy (SERS) to access oxidized cytC heme in intact mitochondria with functional ETC[26].

SERS is a highly effective tool to assess the structure of molecules based on their specific vibrational modes. SERS utilizes strong electromagnetic fields obtained due to surface plasmon resonance (SPR)[27,28]. Plasmon nanostructures allow for the detection of molecules at very low, of the order of nM, concentrations[29,30]. The spectral position of SPRs can be tuned by the geometry, composition, size, and shape of nanoparticles[31,32]. SERS is widely used in biochemistry, pharmacology, and biomedical sciences[33,34]. We showed that mitochondria suspension placed on Ag nanostructured surface gives an intensive SERS spectrum corresponding to SERS spectrum of cytC heme[26]. Using purified wild type cytC and its mutant forms we demonstrated that SERS is highly sensitive to the planar/ruffled conformations of oxidized heme, which correlates with its ability to accept electrons from complex III[18]. Sun et al. reported similar results for isolated purified reduced cytC molecules[35]: utilizing resonance Raman spectroscopy and X-ray analysis they demonstrated that reduced wild type and mutant forms of cytC had different probabilities of planar and ruffled heme conformations with various positions of iron towards pyrrol atoms and different abilities to transfer electrons.

Here we show that (i) SERS is a highly sensitive and selective tool to study the conformational changes of heme of oxidized cytC in living mitochondria and to assess the rate of the electron transport in the respiratory chain and mitochondria redox status and (ii) conformation of cytC heme depends on the inner mitochondrial membrane potential. We suggest that the planar conformation of cytC heme enables its optimal orientation towards the heme of cytochrome *c1* in complex III and optimizes cytC function with respect to ETC activity and ATP synthesis. Our study identifies that cytC heme switches conformation in response to membrane potential to regulate the efficiency of the mitochondrial respiratory chain, thus, linking the mitochondrial respiration to the cell's activity.

Results

Assignment of SERS spectrum

For SERS measurements we used plasmonic Ag nanostructured surfaces (AgNSS) of a complex morphology allowing for strong field enhancement (Supplementary Fig. 1–4). These structures enhance Raman signal from cytC molecules[26] and have no inhibitor effect on mitochondria respiration and ETC function (Supplementary Fig. 5 and 6).

To clarify the origin of the peaks in SERS spectra of mitochondria we compared four preparations: isolated mitochondria (Fig. 1a,b), submitochondrial particles (SMP – vesicles of inverted inner mitochondrial membrane with all ETC complexes, ATP-synthase, and cytC encased inside) (Fig. 1c,d), liposomes made of phosphatidylcholine and cardiolipin with the membrane-bound cytC (Fig. 1e,f), and purified cytC. In the mitochondria, cytC molecules are located closer to AgNSS than other ETC cytochromes (Fig. 1b). On the contrary, in SMPs, the "matrix side" of the inner mitochondrial membrane attaches to AgNSS and, thus, *b*-type and c_1 cytochromes are located closer to AgNSSs than cytC molecules (Fig. 1d). In the liposomes, cytC molecules were encapsulated inside liposomes and bound to the inner membrane surface (Fig. 1f). Each preparation was placed on AgNSS and illuminated with the laser light of wavelength 514 or 532 nm – pre-resonance and resonance conditions for *c*- and *b*-type hemes in cytochromes of ETC (Supplementary Fig. 7). Under these conditions cytC, cytochromes c_1 and b_{low}, b_{high} in complex III and cytochrome *b* in complex II give intensive Raman scattering while *a*-type cytochromes in complex IV do not [2,21,23]. An intensive SERS spectrum of mitochondria was recorded (Fig. 1h, spectrum 1) under experimental protocol that ensures electron donation to ETC through complexes I (by malate and pyruvate) and II (by succinate), and to secure ATP synthesis (by ADP).

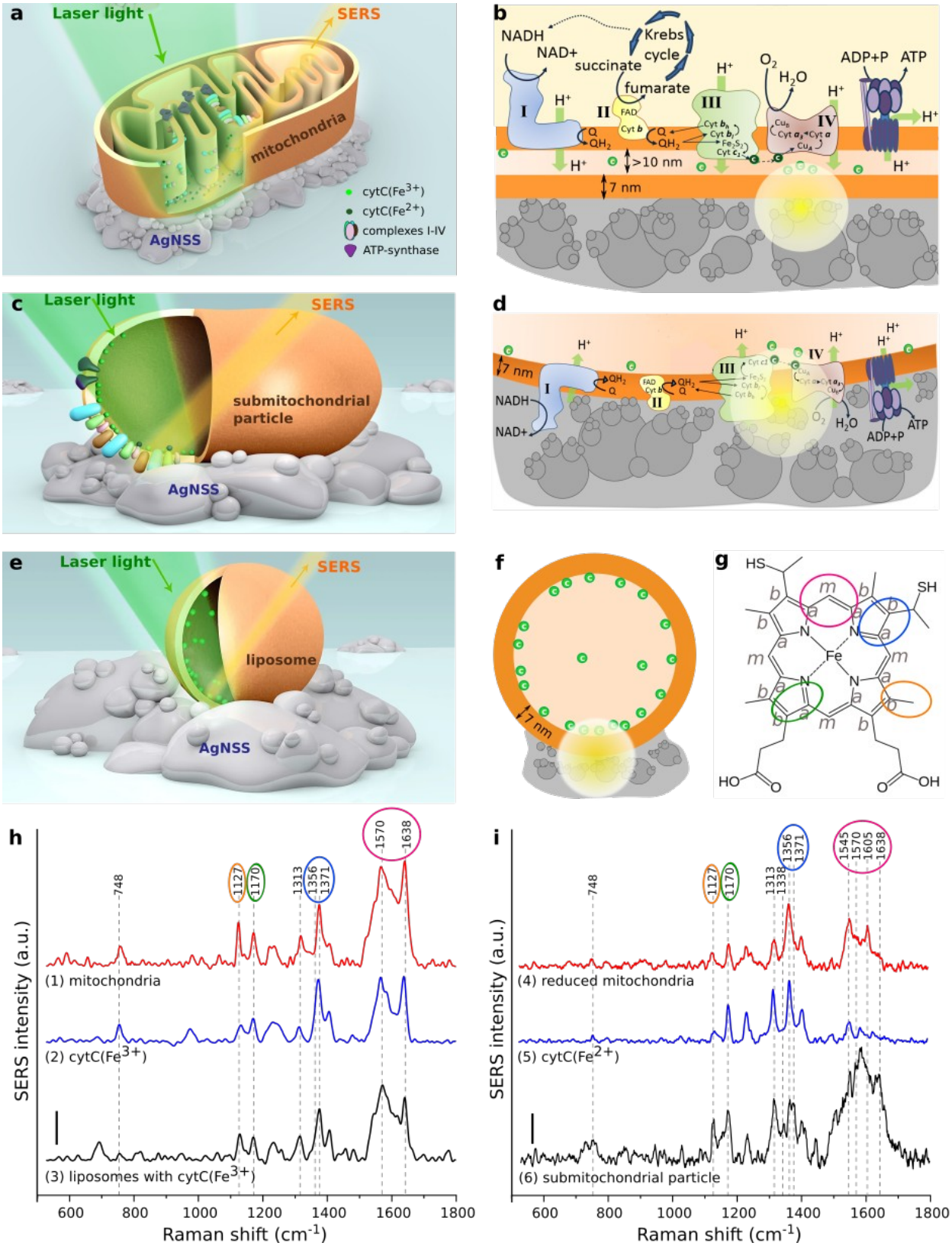

Figure 1. Surface-enhanced Raman scattering from cytochrome *c* molecules in mitochondria, inverted mitochondria, and liposomes. **a, b** Schematic drawing of mitochondria and its submembrane region with

ETC complexes and cytochrome *c* placed on Ag nanostructured surface (AgNSS) illuminated by laser light. SERS originates from oxidized cytC molecules. Oxidized cytC molecules are marked as light green circles; reduced cytC molecules are shown with dark green circles next to complexes III or IV. **c, d** Schematic drawing of a submitochondrial particle (SMP) with ETC complexes and cytC. SERS originates from reduced and oxidized b- and c-types cytochromes. **e, f** Schematic drawing of a liposome containing oxidized cytC bound to the inner membrane surface. **g** Structural formula of a heme *c* molecule. Heme atoms and bonds of interest assessed in SERS spectra are marked in red, blue, orange, and green. **h** SERS spectra of mitochondria, purified oxidized cytC (cytC(Fe^{3+})) and cardiolipin-containing liposomes with internal membrane-bound oxidized cytC (spectra 1–3, respectively). **i** SERS spectra of mitochondria reduced with sodium dithionite, purified reduced cytC (cytC(Fe^{2+})), and submitochondrial particle (spectra 4–6, respectively). SERS spectra 1–3 are normalized by the intensity of the peak at 1371 cm^{-1}; SERS spectra 4–6 are normalized by the intensity of the peak at 1356 cm^{-1}. Vertical bars in **h** and **i** correspond to 1 a.u.

The peak at 1313 cm^{-1} is the characteristic feature of the *c*-type heme (Fig. 1g). This peak is present only in Raman and SERS spectra of *c*-type cytochromes, but not of *b*-type cytochromes[21]. SERS spectrum of mitochondria contains also peaks at 1638 and 1570 cm^{-1} (vibrations of methine bridges between the pyrrole rings), 1371 and 1172 cm^{-1} (symmetric and asymmetric stretching, so-called “breathing” of the pyrrol rings), 1127 cm^{-1} (vibration of C-CH_3 side-radicals) and 748 cm^{-1} (vibration of all heme bonds)[18,20,21,22,23,26,36]. The detailed peak assignment is given in Supplementary Table 1. SERS peaks at 1371 and 1638 cm^{-1} are the “signature” of oxidized, but not reduced, cytochromes (Fig. 1h). The characteristic peaks of reduced cytochromes at 1356, 1545, and 1605 cm^{-1} could be observed only after mitochondria treatment with sodium dithionite that reduces all electron carriers in ETC. The SERS spectrum of mitochondria after sodium dithionite treatment (Fig. 1i, spectrum 4) is similar to the SERS spectrum of reduced cytC (Fig. 1i, spectrum 5). SERS spectra of mitochondria do not contain the characteristic peak (1338 cm^{-1}) of *b*-type cytochromes of complexes II and III. We assume that the absence of peaks assigned to b-type cytochromes and reduced cytochrome *c* is due to the fact that they are located further away from AgNS than cytC is.

To test this we performed SERS experiments on SMP where *b*-type cytochromes are located closer to AgNSS than cytC molecules. SERS spectra of SMP have characteristic peaks at 1313 cm^{-1} (*c*-type heme) and 1338 cm^{-1} (*b*-type heme) (Figs. 1i spectrum 6) and a peak at 1356 cm^{-1} corresponding to reduced hemes (Fig. 1i, spectra 4-6). This means that the enhancement of Raman scattering occurs from both redox forms and both *c*- and *b*-type cytochromes since they are located close to AgNSS. These experimental data are consistent with our suggestion that SERS spectra of functional mitochondria correspond to oxidized cytC: oxidized cytC is located closer to AgNSS than reduced cytC and oxidized/reduced cytB are. The oxidized cytochrome *c1* bound to complex III does not contribute to mitochondria SERS spectra since it is located even further away from AgNSS than reduced cytC is. We suggest that oxidized cytC performs 3D diffusion in the mitochondrial IMS in contrast to reduced cytC that moves along the IMM and complexes III, IV in the supercomplex of respirasome. Such confined movement of the reduced cytC along a particular route between its binding sites in complexes III and IV on the surface of respirasome was discussed[37] but to the best of our knowledge, has never been observed experimentally in intact mitochondria. Due to 3D diffusion oxidized cytC molecules come closer to the outer mitochondrial membrane and AgNSS than reduced cytC molecules do; this enables SERS signal only from oxidized cytC.

To estimate changes in the conformation of cytC heme we used the peak at 1638 cm^{-1} – a signature of the planar heme conformation corresponding to the in-plane vibrations of methine bridges CaCm (Fig. 1g)[17, 36]. Intensity of this peak increases with increasing probability of planar heme conformation and decreases with the increasing probability of ruffled heme conformation[17, 36]. The peak at 1371 cm^{-1} corresponds to symmetric pyrrol half-rings vibrations (so-called v4 vibrations) in oxidized cytC. The v4 pyrrol half-ring vibrations depend only on the redox state of the Fe atom: the corresponding Raman peak at 1371 cm^{-1} originates from the oxidized cytC while the peak at 1356 cm^{-1} corresponds to the reduced cytC. In the

oxidized cytC the intensity of the peak at 1371 cm^{-1} remains constant under changes in heme conformation and, therefore, we use it for normalization. The ratio I_{1638}/I_{1371} can serve as a qualitative estimation of the probability of the planar heme conformation. We also used the ratios I_{1170}/I_{1371} and I_{1170}/I_{1127} to evaluate the probability of the asymmetric vs. symmetric pyrrol half-ring vibrations and the probability of vibrations of heme CH_3-radicals. Previously we demonstrated that these ratios are sensitive to the conformational mobility of protein in the heme surrounding that can affect heme conformation[18].

Proton gradient affects conformation of cytC heme

$\Delta\Psi$ is strongly influenced by the changes in the proton gradient across the inner mitochondrial membrane. Application of pyruvate, malate and succinate (used in the Krebs cycle) and ADP to mitochondria ensures electron transfer along ETC resulting in O_2 reduction to H_2O and in ATP synthesis by ATP-synthase driven by the transmembrane proton gradient created during the electron transport (Fig. 2a). To dissipate the H^+-gradient we applied protonophore CCCP – a highly selective H^+-ionophore that incorporates into the IMS and transfers protons from the intermembrane space to the mitochondrial matrix. This diminishes proton gradient on IMM, increases pH of the intermembrane space, and decreases $\Delta\Psi$; the respiratory chain begins to work more intensively, transferring electrons faster in order to restore the proton gradient and membrane potential (Fig. 2a)[38]. This is manifested in SERS spectra of mitochondria through an increased intensity in the region 1500–1700 cm^{-1} (Fig. 2b, spectrum 3) compared to the original SERS spectrum of mitochondria after substrate application (Fig. 2b, spectrum 2). An increase in the ratio I_{1638}/I_{1371} after CCCP application (Fig. 2c) corresponds to the increased probability of methine bridges vibrations (C_aC_m, C_aC_mH bonds, Fig. 1g) in comparison with symmetric vibrations of pyrrol half-rings in the oxidized cytC heme. This is associated with an increased in-plane mobility of the cytC heme and a higher probability of the planar conformation of heme that favors a higher rate of electron transfer. We did not observe significant changes in the ratios I_{1170}/I_{1371} and I_{1170}/I_{1127} . This indicates the absence of changes in vibrations of CH_3-radicals and

asymmetric vibrations of pyrrol half-rings, and hence in the conformational mobility of the proteins surrounding the heme molecule (Fig. 2d,e). CCCP did not cause changes in the ratio I_{1638}/I_{1371} when applied after rotenone that prevents the accumulation of protons in the intermembrane space due to the selective inhibition of complex I (Fig. 2f): CCCP effect on the cytC heme conformation is observed only when the proton gradient across IMM is established. On the contrary, a decline in the ratio I_{1638}/I_{1371} was observed after the application of oligomycin that inhibits ATP-synthase and leads to the accumulation of protons in the intermembrane space of mitochondria, to the hyperpolarization of IMM, and to the slow-down of ETC (Fig. 2g). The decreased ratio I_{1638}/I_{1371} corresponds to the decreased in-plane mobility, a lower probability of the planar heme conformation, and a higher probability of the deformed, ruffled heme. The subsequent application of CCCP that transfers protons from the IMS to the mitochondrial matrix and restores ETC activity led to an increase in the ratio I_{1638}/I_{1371} in oligomycin-treated mitochondria (Fig. 2g). Moreover, we detected an increase in the ratio I_{1638}/I_{1371} with the increase in pH of the physiological buffer used for mitochondria (Fig. 2h). Neither rotenone, nor oligomycin, nor extramitochondrial pH affected other peak ratios (Supplementary Fig. 8). The spectra of isolated purified cytC were not influenced by pH, which is associated with the absence of direct effect of proton gradient on the heme conformation of purified cytC in the solution (Supplementary Fig. 9). Our results confirm that the disappearance or restoration of electrochemical proton gradient in mitochondria affects cytC heme conformation not via direct interaction of protons with cytC but due to complex processes mediated by $\Delta\Psi$ changes.

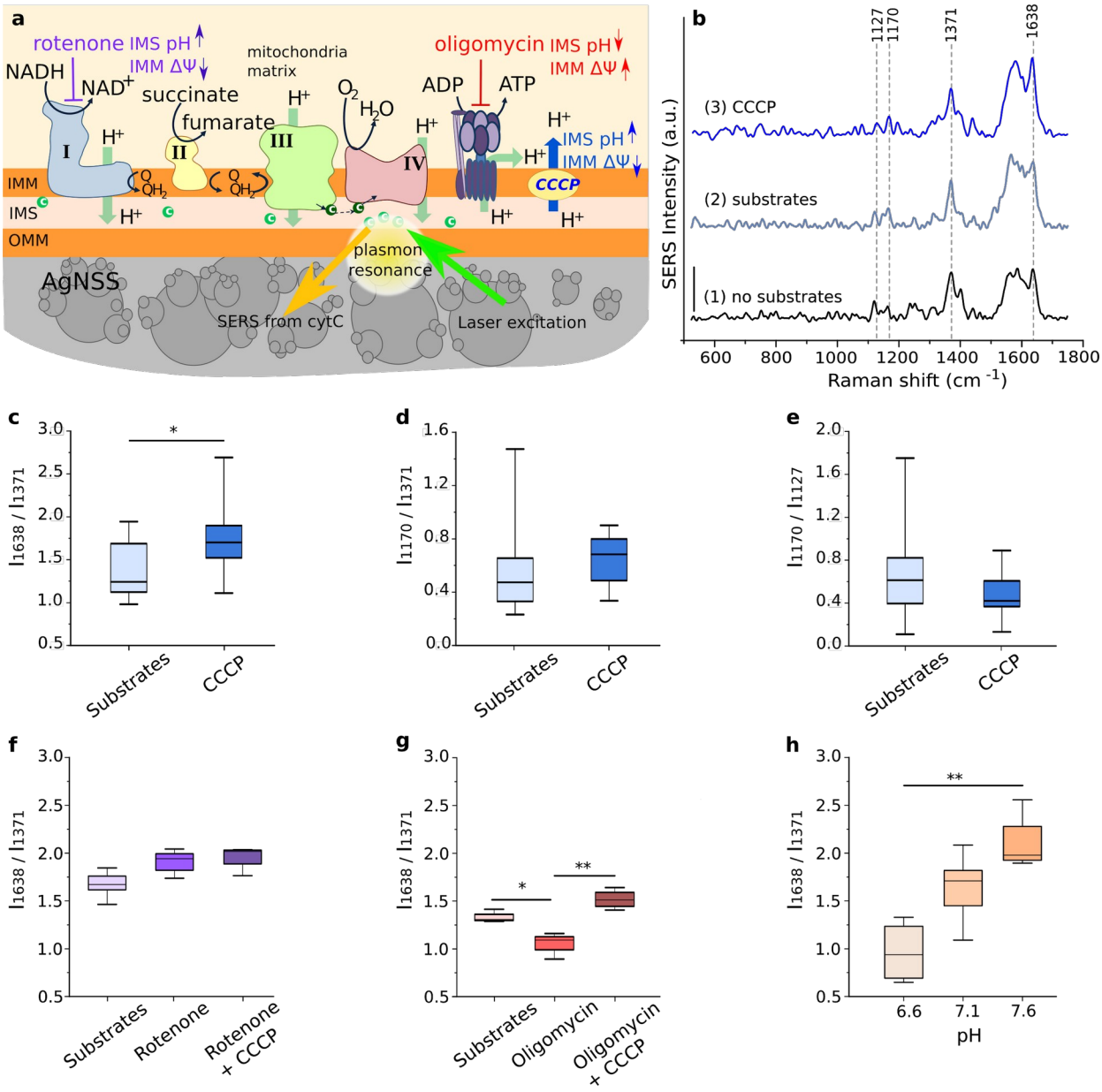

Figure 2. Proton gradient affects the conformation of cytC heme. a Schematic drawing of mitochondria on Ag nanostructured surface (AgNSS): outer and inner membranes (OMM and IMM), intermembrane space (IMS), ETC complexes, oxidized and reduced cytochrome *c* molecules (light and dark green circles in IMS), and sites of rotenone, oligomycin and CCCP action. **b** SERS spectra of mitochondria before and after application of ETC substrates (malate, pyruvate, succinate, and ADP), and after CCCP treatment (0.5 μM) (spectra 1-3, respectively). SERS spectra are normalized by the intensity of the peak at 1371 cm^{-1}. Vertical scale-bar corresponds to 1 a.u. **c–e** The ratios I_{1638}/I_{1371} (the probability of the planar heme conformation), I_{1170}/I_{1371} (probability of the asymmetric pyrrol half-ring vibrations), and I_{1170}/I_{1127} (probability of vibrations of heme CH_3-radicals) before and after CCCP treatment (n=9). **f** The ratio I_{1638}/I_{1371} before and after

application of rotenone (50 nM), and after the following application of CCCP (0.5 μM) (n=4). **g** The ratio I_{1638}/I_{1371} before and after administration of oligomycin (10 μM), and after the following application of CCCP (0.5 μM)) (n=4). **h** Dependence of the ratio I_{1638}/I_{1371} on pH in mitochondrial buffer (n=4). Data in **c-h** are represented as boxplots. All boxplots indicate median (center line), 25th and 75th percentiles (bounds of box), and minimum and maximum (whiskers). *p<0.05, **p<0.01 (Nonparametric Kruskal-Wallis test with Dunn's multiple comparison post-test correction).

Potassium gradient affects conformation of cytC heme

To check whether observed changes in SERS spectra of mitochondrial cytC under modulation of proton transport across IMM are caused by evoked changes in the potential of inner mitochondrial membrane we studied the effect of K^+-ionophore valinomycin (Fig. 3). Valinomycin incorporates into the IMM and transfers K^+ ions from the IMS into the mitochondrial matrix down the electrochemical K^+-gradient resulting in a decrease of ΔΨ (Fig. 3g)[39]. Valinomycin, similar to CCCP, causes an increase in the electron transport rate in ETC in order to restore ΔΨ. We observed an increase in the ratio I_{1638}/I_{1371} under the application of valinomycin (0.1 μM) to the mitochondria suspension with the pyruvate, malate, succinate, and ADP (Fig. 3a, left). Valinomycin, however, does not affect the ratios I_{1170}/I_{1371} and I_{1170}/I_{1127}, which indicates the absence of ΔΨ influence on the vibrations of CH_3-radicals and asymmetric vibrations of pyrrol half-rings and, thus, on the conformational mobility of the protein surrounding of the heme molecule (Figs. 3 b,c, left).

Valinomycin effect on heme conformation depends on the presence of the Krebs cycle substrates and ADP that are essential for the maintenance of the electron transport in ETC and for the formation of ΔΨ on the inner mitochondrial membrane. Valinomycin transfers K^+ ions across the IMM into the mitochondrial matrix only when ΔΨ exists (Fig. 3g). Therefore we did not observe the effect of valinomycin on the ratio I_{1638}/I_{1371} in mitochondria with non-operating ETC (without ETC substrates and ADP in the mitochondrial buffer) (Fig. 3a, right).

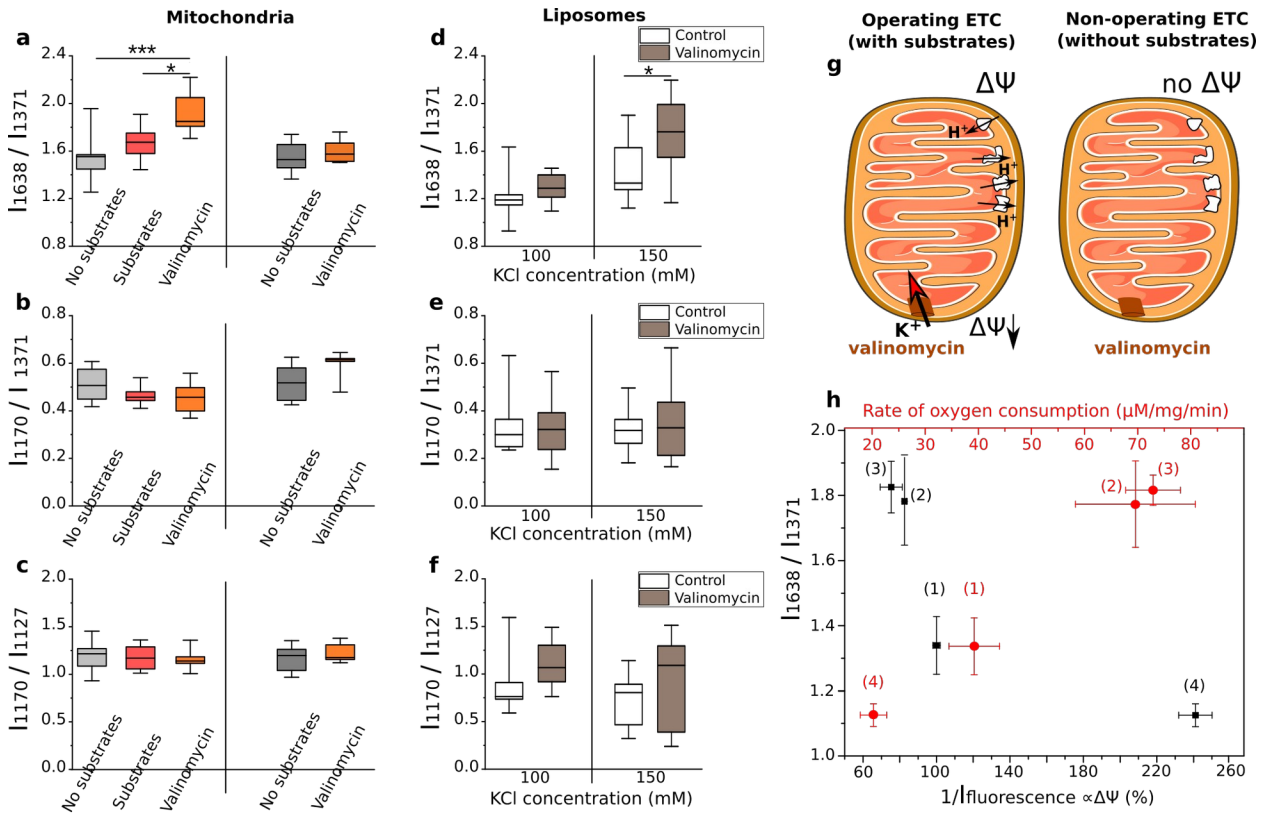

Figure 3. Membrane potential affects the conformation of cytC heme in mitochondria and cardiolipin-containing liposomes. a–c The ratios of peak intensities I_{1638}/I_{1371} (the probability of the planar heme conformation), I_{1170}/I_{1371} (probability of the asymmetric pyrrol half-ring vibrations), and I_{1170}/I_{1127} (probability of vibrations of heme CH_3-radicals) calculated from SERS spectra of mitochondria **(left panel)** with active ETC: without substrates (grey boxes), with substrates – malate, pyruvate, succinate and ADP (red boxes), and after following valinomycin application (orange boxes); **(right panel)** with non-active ETC: without substrates (dark grey boxes) and after valinomycin application (orange boxes). **d–f** The ratios I_{1638}/I_{1371}, I_{1170}/I_{1371}, and I_{1170}/I_{1127} calculated from SERS spectra of liposomes before (white boxes) and after valinomycin (1 μM) application (brown boxes) for 100 and 150 mM KCl concentrations in the outside solution. Data in **a–f** are represented as boxplots. All boxplots indicate median (center line), 25th and 75th percentiles (bounds of box), and minimum and maximum (whiskers). *p<0.05, ***p<0.001 (Nonparametric Kruskal-Wallis test with post Dunns multiple comparison). **g** Schematic drawing of mitochondria with and without Krebs cycle substrates and ADP under application of valinomycin. Valinomycin provides inward K^+ transport in mitochondria with operating ETC. **h** Ratio I_{1638}/I_{1371} *vs*. the rate of oxygen consumption by mitochondria (red circles, red X-axis) and *vs.* the inner mitochondrial membrane potential ΔΨ estimated qualitatively as the reverse values of fluorescence intensity of MitoTrackerCMXRos (black squares, black X-axis). The measurements were done under the following conditions: with ETC substrates (state 1), with

the sequential addition of either CCCP (state 2), or valinomycin (state 3), or oligomycin (state 4). Data are represented as mean values and errors of the mean.

To test our hypothesis that CytC heme conformation depends on $\Delta\Psi$ we performed experiments with liposomes made of phosphatidylcholine and cardiolipin and containing cytC inside bound to cardiolipin (Fig. 1e,f). Before SERS measurements liposome samples were diluted with KCl solution to the final K^+ concentrations of 100 or 150 mM. We found that SERS spectra of cytC bound to the inner surface of the liposome membrane do not depend on K^+ concentration in the outside buffer (Fig. 3d–e, white boxes). At the same time we observed a significant increase in the ratio I_{1638}/I_{1371} under valinomycin application when the concentration of KCl in the outside buffer was 150 mM (Fig. 3d). This indicates an increased probability of the planar heme conformation. The relative intensities of other SERS peaks did not change, which designates the absence of the valinomycin influence on pyrrol rings and CH_3-side radicals (Fig. 3e–f). We did not observe any effect of K^+ ions without or with valinomycin on SERS spectra of cytC bound only to the outer surface of the membrane of cardiolipin-containing liposomes (Supplementary Fig. 10). These results reveal that cytC heme conformation is sensitive to processes in the confined close-to-membrane spaces evoked by K^+ transport through the membrane: changes in the local electromagnetic field, redistribution of surface charges and submembrane ions. We suggest that in mitochondria with functional ETC – where the intermembrane space is only 2-4-folds bigger than the cytC diameter and where conditions are closed to those described in the “crowding molecules” theory[40] – the effect of ions, membrane surface charge, and local electro-magnetic field on cytC heme conformation can be greater than that in liposomes and in solutions with purified isolated cytC molecules.

To demonstrate the relation between conformational changes in cytC heme and mitochondria activity we measured oxygen consumption by mitochondria under normal ETC function (with malate, pyruvate, succinate, and ADP application), under ETC activation CCCP or valinomycin application) or under ETC

inhibition (oligomycin application). With the increased ETC activity (the increased oxygen consumption), SERS spectra demonstrate higher values of the ratio I_{1638}/I_{1371}; this corresponds to the higher probability of the planar cytC heme conformation (Fig. 3h, red symbols, states 2 and 3 compared to state 1). Under the decreased ETC activity (reduced oxygen consumption) the ratio I_{1638}/I_{1371} decreases, which corresponds to the higher probability of the ruffled heme conformation (Fig. 3h, red symbols, state 4 compared to state 1). We also performed qualitative estimation of the IMM potential with the fluorescent dye MitoTrackerCMXRos to show directly correlation between ΔΨ and heme conformations. Our data confirmed that IMM depolarization evoked by CCCP or valinomycin results in the increase in the probability of the planar conformation of cytC heme (Fig. 3h, black symbols, states 3 and 4 compared to state 1).

In summary, our data verify that under conditions of the increased ETC activity, which evokes depolarization of inner mitochondrial membrane and dissipation of proton gradient, the cytC heme has an increased in-plane mobility and higher probability of planar conformation. This favors heme *c* orientation towards heme *c1* in complex III, speeds-up ETC and restores ΔΨ and H^+ gradient.

Discussion

We offered a unique SERS-based assessment of conformation changes of cytochrome *c* and their functional outcomes in living mitochondria. SERS of living mitochondria originates from oxidized cytC molecules that diffuse between inner and outer mitochondrial membranes in IMS and can come to close proximity to AgNSS. SERS from reduced cytC or b-type cytochromes was not detected due to a longer distance between them and AgNSS. To determine a marker of cytC conformational changes we assessed the probability of the planar heme conformation (the ratio I_{1638}/I_{1371} in SERS spectra), the probability of the asymmetric pyrrol half-ring vibrations (the ratio I_{1170}/I_{1371}), and the probability of vibrations of heme CH3-radicals (the ratio

I_{1170}/I_{1127}). We identified the ratio I_{1638}/I_{1371} as a reliable marker to monitor electron transport in ETC of living mitochondria.

Our findings suggest that heme of oxidized cytC in functional mitochondria changes its conformation under depolarization and hyperpolarization of the inner mitochondrial membrane: the probability of the planar heme conformation significantly increases under IMM depolarization induced by CCCP and valinomycin, under pH increase, and decreases under IMM hyperpolarization induced by the inhibition of ATP synthase (Fig. 2c,g,h; Fig. 3a). There are at least two possibilities of ΔΨ effect on cytC heme: (i) via phosphorylation of the Tyr-residues of cytC by specific ΔΨ -dependent kinase in the IMS or/and (ii) via a direct effect of the local electromagnetic field. Many studies demonstrated the existence of ΔΨ-dependent cytC-kinase in IMS that is activated under high ΔΨ resulting in cytC phosphorylation and a decrease in cytC activity[14,15]. We suggested that phosphorylation of cytC under high ΔΨ results in a decrease in the probability of the planar heme conformation, whereas inactivation of the cytC kinase under IMM depolarization causes a gradual dephosphorylation of cytC and the increased probability of planar conformation of cytC heme. The direct effect of ΔΨ on cytC heme can be due to the "crowding molecules" condition[40]: being located between outer and inner mitochondrial membranes cytC is affected by changes in (i) local concentration of protons,membrane potential, and surface charge distribution, (ii) in local gradients of Ca^{2+} and K^{+} ions and in the overall ionic strength, etc. According to the theory of crowding molecules[40] cytC in living mitochondria can be much more sensitive to the surroundings than in diluted samples of isolated cytC or in samples of purified cytC with isolated ETC complexes. Our experiments on liposomes with cardiolipin-bound cytC revealed the same changes as in mitochondria under valinomycin application, showing a sensitivity of cytC heme to the transmembrane K^{+}-transport and change in the membrane potential without any enzyme-dependent phosphorylation (Fig. 3d).

We proposed a concept that links the conformation of the cytC heme to ETC activity (Fig. 4). An increased cell activity (top panel) requires higher ATP consumption leading to a decrease in the ratio [ATP]/[ADP]. This causes activation of mitochondrial ATP synthase that utilizes H^+ from the mitochondrial intermembrane space, which results in the dissipation of H^+ gradient and IMM depolarization. CytC senses the IMS surrounding and the CytC heme conformation changes: the probability of the planar conformation increases. Such conformation favors its orientation towards heme in cytochrome *c1* providing electron tunneling and, thus, facilitating the electron transfer between cytochrome *c1* in complex III and cytC. This increases the rate of the overall electron transport in ETC and provides H^+ gradient necessary for the operation of ATP-synthase and optimal synthesis of ATP to meet cellular needs for energy. Fast electron acceptance from complex III by cytC also protects mitochondria from the increased superoxide anion (O_2^-) production in complex III. Vice versa, when a cell decreases its activity (bottom panel) and consumes less ATP, ATP consumption declines and the ratio [ATP]/[ADP] increases, which leads to the inhibition of ATP synthase, accumulation of H^+ in the mitochondrial intermembrane space and IMM hyperpolarization. This affects cytC resulting in an increase in the probability of ruffled heme conformation and in a decrease in the electron transport rate between cytC and complex III, which influences the ETC activity. This leads to a dissipation of the H^+ gradient and a decrease in the ATP-synthase activity producing less ATP to meet energy demands of the cell. When the cell activity rises again the regulatory cycle repeats (the top panel in Fig.4).

The cytC heme-regulated switch enables a cell to match mitochondrial respiratory chain activity to the cell's needs for energy. The conformational and functional insights revealed in this study will be instrumental for a better understanding of cytC function and will bridge a knowledge gap by providing non-invasive, label-free assessment of cellular bioenergetics at early-stage pathologies.

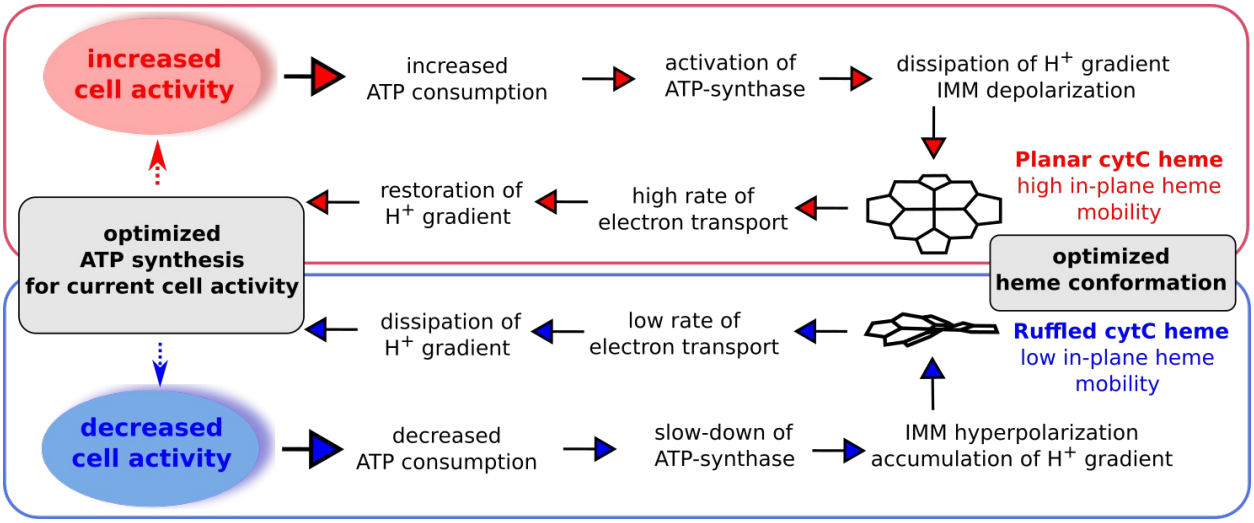

Figure 4. Link between cytC heme conformation and ETC activity to optimize ATP synthesis. Diagram showing the relations between cell activity, ATP consumption, inner mitochondrial membrane potential, cytC heme conformation, and ETC activity essential for the maintenance of the ATP synthesis. CytC heme can switch between planar and ruffled conformations depending on IMM potential to meet cellular needs for energy.

Methods

Mitochondria isolation

Mitochondria were isolated from hearts of male Sprague-Dawley rats, body weight 275–350 g (M&M Taconic, Denmark) and male WKY rats, body weight 280–380 g (BIBCh, Pushchino, Russia)[26]. We did not observe any differences in SERS spectra of mitochondria of these strains. The animal studies were conformed with the Recommendations of the European Laboratory Animal Science Associations 2014 (FELASA) and Danish legislation governing animal experimentation, 1987, and were carried out after permission had been granted by the Animal Experiments Inspectorate, Ministry of Justice, Denmark and by Bioethics Committee of Moscow State University (protocol №82-O, 08.06.2017). Isolated mitochondria were kept in MSTP-buffer (225 mM mannitol, 75 mM sucrose, 20 mM Tris base, 2 KH_2PO4, and 0.5 mM EDTA, pH 7.1) at 4 °C. The concentration of total protein in the obtained mitochondrial sample was 4.5–8 mg/ml. SERS experiments were performed within 2 h after mitochondria isolation.

Liposome preparation

Liposomes with the internally bound cytC were obtained using a standard protocol: https://www.sigmaaldrich.com/technical-documents/articles/biology/liposome-preparation.html. Phosphatidylcholine (Sigma) and cardiolipin (Avanti Polar Lipids) were mixed in the ratio 4:1 by weight and diluted in chloroform in a round bottom flask to the final lipid concentration of 10 mg/ml. The solvent was removed by the rotary evaporation with a vacuum pump at 30 ºC for 30 min. Lipid films were rehydrated in an equal volume of 5 mg/ml cytochrome *c* (Sigma Aldrich) in the buffer (50 mM Tris-Cl, 0.1mM EDTA, pH 7.4) at 30 °C for 30 min. The lipid-protein solution was removed from the flask after the exposure to ultrasonic bath for 5 min. The solution was then sonicated five times for 30 s with an interval of 30 s to remove lipid-protein complex aggregates. The suspension was disrupted by seven freeze-thaw cycles in liquid nitrogen followed by eleven cycles of extrusion through a filter with 100 nm pores (Avanti Mini-Extruder). Potassium chloride was added to the final concentration of 100 mM. External cytochrome *c* was removed by size exclusion chromatography with Sephadex G150 in the buffer (50 mM Tris-Cl, 0.1 mM EDTA, 100 mM KCl, pH 7.4).

Liposomes with cytC bound to the outer surface of liposome membrane were obtained by the same protocol with the only difference that lipid films were rehydrated in the equal volume of 50 mM Tris-Cl buffer with 0.1mM EDTA (pH 7.4) at 30 °C for 30 min (without cytC). After eleven cycles of extrusion through a filter with 100 nm pores cytC was added to liposomes to the final concentration of 2.2 μM and incubated at 20 °C for 30 min to insure cytC binding to cardiolipin of the outer liposome surface.

Submitochondrial particle preparation

Inside-out submitochondrial particles (SMP or inverted mitochondria) were prepared from bovine heart, activated, and coupled by treatment with oligomycin (0.5 μg/mg of SMP protein), as described[41]. Respiratory control ratio with NADH was 6.5 indicating a functional ETC.

AgNSS synthesis

AgNSSs were fabricated by ultrasonic silver rain procedure as described in[26,42] with modifications. Briefly, 2.93 g of silver nitrate (Sigma, 99.999% purity) was dissolved in 100 ml of MilliQ water under constant stirring. 7 g of NaOH were diluted in 30 ml of MilliQ and poured into the $AgNO_3$ solution. The obtained dark precipitate was washed three times with 100 ml of MilliQ water. 7 ml of 10% ammonia aqueous solution was added to dissolve the precipitated; an additional 25 ml volume of the 10% ammonia solution was added. The final volume of the solution was adjusted to 170 ml with MilliQ . The temperature of the coverslips were maintained at 340 °C (magnetic stirrer with heating IKA C-MAG HS 4 digital) during the experiment and 15 min after. The solution of silver ammonia complex was sprayed onto the entire surface of coverslips (using Albedo ultrasonic nebulizer) for an hour with 5-min breaks every 3–4 min. The coverslips were stored in the dark at room temperature.

AgNSS characterization

SEM and TEM measurements were done by NVision 40 electron microscope (Carl Zeiss) with 7 kV accelerating voltage and LEO912 AB OMEGA microscope (Carl Zeiss), respectively.

Optical characterizations were performed on a BX51 microscope (Olympus) equipped with a halogen light source, polarizers, and a fiber-coupled grating spectrometer QE65000 (Ocean Optics) with a wavelength resolution of 1.6 nm. The reflected light was collected in backscattering configuration using MPlanFL (Olympus) objectives with magnifications ×100 (NA =0.9).

In order to reveal and visualize main features of spatial distribution of hot spots, we used a scattering-type scanning near-field optical microscope (s-SNOM) ("NeaSNOM" by Neaspec GmbH) based on an atomic force microscope (AFM) that uses cantilevered Si tips covered with platinum as near-field probes[43]. The sample was scanned in a tapping mode, with the tip oscillating at the mechanical resonance frequency $\Omega \approx$ 250 kHz with an amplitude ∼50 nm. The tip-sample interface was illuminated under 50° relative to the sample surface by a linearly *P*-polarized tunable (1480–1625 nm) telecom laser. The experimental conditions matched numerical simulations of a strong electric near-field in a system of AgNSS[26].

Raman spectroscopy measurements

Confocal Raman microspectrometers InVia Raman (Renishaw, UK) with 514 nm and 532 nm lasers were used to acquire SERS spectra of mitochondria, isolated purified cytC, SMP and liposomes with cytC. Excitation and collection of SERS signal were done via objective 20x, NA 0.4 with laser power 1.5 mW per excitation spot with 0.5–1 μm diameter. Accumulation time for each SERS spectrum was 20 s.

SERS measurements of mitochondria

Before SERS experiments the initial mitochondrial sample (30 μl) was diluted with the physiological phosphate-based solution (150 mM KCl, 5 mM Tris-HCl, 1 mM EGTA, 5 mM Na2HPO4, 1.5 mM CaCl2, pH 7.1, 4 °C); this resulted in the experimental mitochondrial sample with the total protein concentration of 0.1 mg/ml. Sodium pyruvate (2 mM), sodium succinate (5 mM), ADP (2 mM) and $MgCl_2$ (3 mM) were added to ensure electron transfer in ETC and to stimulate ATP synthesis by complex V. 300 μl of the experimental mitochondrial sample were dropped on an AgNSS placed in a MatTek glass bottom dish; SERS spectra of mitochondria with substrates (pyruvate, malate, succinate, and ADP) were recorded within 30–60 s. SERS spectra of mitochondria after the application of either protonophore CCCP (0.5 μM), or K^+-

ionophore valinomycin (0.1 μM), or oligomycin (10 μM) plus CCCP (0.5 μM), or rotenone (1 μM) plus CCCP (0.5 μM) (Sigma) were recorded within 2 min.

To study the effect of H^+ on SERS spectra of cytC in mitochondria the initial mitochondrial sample was diluted with the phosphate-based solutions with different pH (6.1, 6.6, 7.1, and 7.6). We used 514 nm laser in the experiments with CCCP, valinomycin, and pH while 532 nm laser was used in the experiments with rotenone, rotenone plusCCCP, oligomycin, and oligomycin plus CCCP. We demonstrated that (i) experimental protocols and AgNSS did not affect mitochondria respiration and membrane integrity (Supplementary Fig. 5) and (ii) SERS spectra of mitochondria remain efficient and stable over time and along SERS substrates[26].

SERS measurements of liposomes

To record SERS spectra of cytC bound to the inner surface of cardiolipin-containing liposomes the initial liposome samples were diluted twice with K^+-containing phosphate buffer to obtain liposome samples with the final K^+ concentration of 100 and 150 mM. 300 μl of the solution with liposomes were placed into a MatTek glass bottom dish with AgNSS. SERS spectra of liposomes were obtained at laser excitation wavelength of 514 nm.

SERS and Raman measurements of purified cytC

To record SERS spectra of isolated purified oxidized cytC (Sigma) was diluted with PBS (pH 7.2) to the final concentration of 10^{-6} M. 300 μl of cytC solution were dropped into a MatTek glass bottom dish with AgNSS. SERS spectra of cytC were obtained at laser excitation wavelength of 514 nm. To record Raman spectra of isolated purified oxidized cytC at different pH values the cytC was diluted with PBS with different pH (5.0, 6.0, 7.5, and 8.0) to the final concentration of 1 mM. 300 μl of cytC solution were

dropped into a MatTek glass bottom dish. Raman spectra of cytC were obtained at laser excitation wavelength of 532 nm. Excitation and collection of Raman scattering was done via objective 20x, NA 0.4 with laser power 1.5 mW per excitation spot with 0.5–1 μm diameter, spectrum accumulation time was 20 s. The study of pH effect on heme of oxidized cytC was done by means of resonance Raman spectroscopy, not SERS, to avoid possible effect of high H^+ concentrations on plasmonic properties of AgNSSs.

SERS measurements of submitochondrial particle

Preliminary obtained samples of SMPs were defrosted, NADH (0.1 mM) was added and 300 μl of SMP solution was placed into Mattek glass bottom dish with AgNSS. SERS spectra of SMPs were obtained at laser excitation wavelength of 514 nm.

Spectrum analysis

SERS and Raman spectra were processed using open source software Pyraman available at https://github.com/abrazhe/pyraman. The baseline was subtracted in each spectrum. It was defined as a cubic spline interpolation of a set of knots, number and x-coordinates of which were selected manually outside any informative peaks in the spectra. Number and x-coordinates of the knots were fixed for all spectra in the study. Y-coordinates of the knots were defined separately for each spectrum as 5-point neighborhood averages of spectrum intensities around the user-specified x-position of the knot. The baseline subtraction parameters were chosen after preliminary processing of a randomly selected set of approximately 40 spectra from different preparations to ensure that all typical baseline variations were taken into account. To compare changes in SERS spectra on various stimuli we calculated the ratios of peak intensities I_{1638}/I_{1371}, I_{1170}/I_{1371}, I_{1170}/I_{1127} after the baseline subtraction.

Oxygen consumption rate measurement

Oxygen consumption by mitochondria was measured with the Clark-type electrode using oximeter Expert001.MTX ("Econics", Russia). Mitochondria were injected into the thermostatic chamber (24 ^{o}C) with MSTP-buffer to achieve final concentration of total protein of 0.1 mg/ml. MSTP-buffer and solutions of malate, pyruvate, succinate, ADP, CCCP, valinomycin, and oligomycin were kept in open flasks at 24 ^{o}C at least one hour before the experiments. Substrates and uncoupling agents were injected into the chamber consistently when the oxygen consumption rate reached a steady state. The rate of oxygen consumption by mitochondria was measured according to Chance's method with modifications[38].

Measurements of mitochondrial membrane potential

For the measurement of mitochondrial membrane potential ($\Delta\Psi$), mitochondria were stained with the potential-sensitive fluorescent dye MitoTrackerCMXRos (ThermoFisher). The MitoTrackerCMXRos dye is known to accumulate in mitochondria proportionally the value of $\Delta\Psi$ with the concentration self-quenching of its fluorescence[44]. Fluorescence spectra of mitochondria were recorded by Raman microspectrometer NTEGRA SPECTRA (NT-MDT, Russia) with the laser excitation wavelength of 532 nm, grating 150 lines/mm and laser power at the exit from the objective (x5, NA 0.15) of 0.05 mW. The accumulation time of one spectrum was 10 s. The fluorescence intensity of the MitoTrackerCMXRos was determined as the intensity of the fluorescence peak at the wavelength of 610 nm.

Isolated mitochondria were diluted with MSTP-buffer containing ETC substrates and MitoTrackerCMXRos dye (100 nM). They were incubated in the dark at room temperature for 15 min. Total protein concentration in the incubated mitochondria sample was 2 mg/ml. The suspension of mitochondria was centrifuged at 7000g, 4°C for 10 min. The supernatant was removed, the sediment homogenized and resuspended with MSTP buffer containing ETC substrates without MitoTrackerCMXRos dye and centrifuged at 7000g, 4 °C

for 10 min. The supernatant was removed and the pellet was resuspended in 500 µl of MSTP-buffer until a homogeneous mitochondria sample was obtained. We recorded fluorescence spectra of the mitochondrial samples with ETC substrates, with the sequential addition of CCCP (0.5 µM) or valinomycin (1 µM). To assess the effect of oligomycin on ΔΨ mitochondria were incubated in MSTP-buffer with ETC substrates, MitoTrackerCMXRos dye (100 nM) and oligomycin (10 µM) in the dark for 15 min. For the comparison, another mitochondria sample was incubated in the MSTP-buffer with ETC substrates and MitoTrackerCMXRos dye without oligomycin for 15 min. After the incubation both mitochondria samples were centrifuged two times at 7000g, 4°C for 10 min; after each centrifugation the supernatant was replaced with MSTP-buffer plus substrates plus oligomycin or with MSTP plus substrates. To estimate changes in ΔΨ the reciprocal values of the fluorescence intensity ($1/I_{fluor}$) of mitochondria sample after the application of ionophores or inhibitors were normalized to $1/I_{fluor}$ value of the mitochondria sample with substrates and given in %. An increase in $1/I_{fluor}$ corresponds to the hyperpolarization of the inner mitochondrial membrane while the decrease corresponds to the depolarization of the inner mitochondrial membrane.

Statistics

Data were represented as boxplots. All boxplots indicate median (center line), 25th and 75th percentiles (bounds of box), and minimum and maximum (whiskers). For the statistical analysis we applied a nonparametric Kruskal-Wallis test with Dunns multiple comparison post-test correction. The scatter plots shown on Fig.3h are represented as mean values and error of the mean.

Data availability

The data that support the findings of this study are available from the corresponding author upon reasonable request.

References

(1) Turrens, J.F. Mitochondrial formation of reactive oxygen species. *J. Physiol* **552**, 335–344 (2003).

(2) Wang, G.J, Jackson, J.G,, Thayer, S.A. Altered distribution of mitochondria impairs calcium homeostasis in rat hippocampal neurons in culture. *J. Neurochem*. **87**, 85–94 (2003).

(3) Ježek, P., Hlavata, L. Mitochondria in homeostasis of reactive oxygen species in cell, tissues, and organism. *Int. J. Biochem. Cell Biol*. **37**, 2478–503 (2005).

(4) Genova, M.L., Lenaz, G. Functional role of mitochondrial respiratory supercomplexes. *Biochim. Biophys. Acta* **1837**, 427–443 (2014).

(5) Ow, Y. et al. Cytochrome *c*: functions beyond respiration. *Nat. Rev. Mol. Cell. Biol.* **9**, 532–542 (2008).

(6) Moreno-Beltrán, B. et al. Structural basis of mitochondrial dysfunction in response to cytochrome c phosphorylation at tyrosine 48. *PNAS* **114**, E3041–E3050 (2017).

(7) Foti, S.C. et al. Cerebral mitochondrial electron transport chain dysfunction in multiple system atrophy and Parkinson's disease. *Sci. Rep.* **9,** 6559 (2019).

(8) Lapuente-Brun, E. et al. Supercomplex assembly determines electron flux in the mitochondrial electron transport chain. *Science* **340,** 1567–70 (2013).

(9) Lopez-Fabuel, I. et al. Complex I assembly into supercomplexes determines differential mitochondrial ROS production in neurons and astrocytes. *Proc. Natl. Acad. Sci. USA* **113**, 13063–13068 (2016).

(10) Huttemann, M. et al. The multiple functions of cytochrome c and their regulation in life and death decisions of the mammalian cell: From respiration to apoptosis. *Mitochondrion.* **11**, 369–81 (2011).

(11) Ow, Y. et al. Cytochrome c: functions beyond respiration. *Nat. Rev. Mol. Cell Biol*. **9**, 532–542 (2008).

(12) Huttemann, M. et al. Phosphorylation of mammalian cytochrome c and cytochrome c oxidase in the regulation of cell destiny: respiration, apoptosis, and human disease. *Adv. Exp. Med. Biol.* **748**, 237–64 (2012).

(13) Bushnell, G.W., Louie, G.V., Brayer, G.D. High-resolution three-dimensional structure of horse heart cytochrome c. *J. Mol, Biol*. **214**, 585–95 (1990).

(14) Lee, I. et al. New prospects for an old enzyme: mammalian cytochrome c is tyrosine-phosphorylated in vivo. *Biochem*. **45**, 9121–9128 (2006).

(15) Zhao, X. et al. Phosphoproteome analysis of functional mitochondria isolated from resting human muscle reveals extensive phosphorylation of inner membrane protein complexes and enzymes. *Mol. Cell. Proteomics. Bioenergetics*, **10**, M110.000299 (2010).

(16) Lee, I., Salomon, A.R., Yu, K, Doan, J.W, Grossman L.I, Hüttemann M. New prospects for an old enzyme: mammalian cytochrome c is tyrosine-phosphorylated in vivo. *Biochem.* **45**, 9121–8 (2006).

(17) Ma, J.G. et al. Shelnutt he Structural Origin of Nonplanar Heme Distortions in Tetraheme Ferricytochromes c3. *Biochem.* **37**, 12431–12442 (1998).

(18) Chertkova, R.V. et al. New insight into the mechanism of mitochondrial cytochrome c function *PloS One*. **12**, e0178280 (2017).

(19) Wackerbarth, H., Hildebrandt, P. Redox and Conformational Equilibria and Dynamics of Cytochrome c at High Electric Fields. *Chem. Phys.Chem*. **4**, 714–724 (2003).

(20) Berezhna, S. et al. Resonance Raman Investigations of Cytochrome c Conformational Change upon Interaction with the Membranes of Intact and Ca2 -Exposed Mitochondria. *Biochem.* **42**, 6149–6158 (2003).

(21) Ogawa, M. et al. Label-free biochemical imaging of heart tissue with high-speed spontaneous Raman microscopy. *Biochem. Biophys. Res. Comm*. **382**, 370–374 (2009).

(22) Brazhe, N. et al. In Situ Raman Study of Redox State Changes of Mitochondrial Cytochromes in a Perfused Rat Heart. *PloS One*. **8**, e70488 (2013).

(23) Okada, M. et al. Label-free Raman observation of cytochrome c dynamics during apoptosis. *PNAS J.* **109**, 28–32 (2012).

(24) Love, D.T. et al. The role of the myeloperoxidase-derived oxidant hypothiocyanous acid (HOSCN) in the induction of mitochondrial dysfunction in macrophages. *Redox Biology* **36**, 101602 (2020).

(25) Perry, D.A. et al. Responsive monitoring of mitochondrial redox states in heart muscle predicts impending cardiac arrest. *Science Translational Medicine* **9**, eaan0117 (2017).

(26) Brazhe, N. et al. Probing cytochrome c in living mitochondria with surface-enhanced Raman spectroscopy. *Sci. Rep.* **5**, 13793 (2015).

(27) Maier, S.A. Plasmonic field enhancement and SERS in the effective mode volume picture. *Opt. Express* **14**, 1957–1964 (2006).

(28) Gramotnev, D.K., Bozhevolnyi, S.I. Plasmonics beyond the diffraction limit. *Nat. Photonics* **4**, 83. (2010).

(29) Kneipp, J., Kneipp, H., Kneipp, K. SERS - a single-molecule and nanoscale tool for bioanalytics. *Chem. Soc. Rev*. **37,** 1052–1060 (2008).

(30) Huang, J., et al. SERS discrimination of single DNA bases in single oligonucleotides by electro-plasmonic trapping. *Nat. Commun.* **10**, 5321 (2019).

(31) Langer, J. et al. Present and Future of Surface-Enhanced Raman Scattering. *ACS Nano* **14**, 28–117 (2020).

(32) Novikov, S.M. et al. Fractal Shaped Periodic Metal Nanostructures Atop Dielectric-Metal Substrates for SERS Applications. *ACS Photonics* **7**, 1708–1715 (2020).

(33) Wang, X. et al. Fundamental understanding and applications of plasmon-enhanced Raman spectroscopy. *Nat. Rev. Phys.* **2,** 253–271 (2020).

(34) Rickard, J.J.S. et al. Rapid optofluidic detection of biomarkers for traumatic brain injury via surface-enhanced Raman spectroscopy. *Nat. Biomed. Eng.* **4**, 610–623 (2020).

(35) Sun, Y. et al. Investigations of heme distortion, low-frequency vibrational excitations, and electron transfer in cytochrome c. *PNAS* **111**, 6570–6575 (2014).

(36) Hu, S. et al. Complete assignment of cytochrome resonance Raman spectra via enzymatic reconstitution with isotopically labelled hemes. *J. Am. Chem. Soc.* **115**, 12446–12458 (1993).

(37) Guerra-Castellano, A. et al. Oxidative stress is tightly regulated by cytochrome c phosphorylation and respirasome factors in mitochondria. *PNAS* **115**, 7955–7960 (2018).

(38) Doerrier, C., Garcia-Souza, L.F., Krumschnabel, G., Wohlfarter Y., Mészáros A.T., Gnaiger E. (2018) High-Resolution FluoRespirometry and OXPHOS Protocols for Human Cells, Permeabilized Fibers from Small Biopsies of Muscle, and Isolated Mitochondria. In: Palmeira C., Moreno A. (eds) Mitochondrial Bioenergetics. Methods in Molecular Biology, vol 1782. Humana Press, New York, NY.

(39) Poppe, M. et al. Dissipation of potassium and proton gradients inhibits mitochondrial hyperpolarization and cytochrome c release during neural apoptosis. *J Neurosci*. **21**, 4551–63 (2001).

(40) Zimmerman, S.B., & Minton, A.P. Macromolecular Crowding: Biochemical, Biophysical, and Physiological Consequences. *Annu. Rev. Biophys. Biomol. Struct*. **22**, 27–63 (1993).

(41) Grivennikova V.G., Gladyshev G.V., Vinogradov A.D. Deactivation of mitochondrial NADH:ubiquinone oxidoreductase (respiratory complex I): Extrinsically affecting factors. *Biochim. Biophys. Acta Bioenerg.* **1861,** 148207 (2020).

(42) Semenova, A. et al. Planar SERS nanostructures with stochastic silver ring morphology for biosensor chips. *J. Materials Chem.* **22**, 24530 (2012).

(43) Zenin, V.A. et al. Boosting local field enhancement by on-chip nanofocusing and impedance-matched plasmonic antennas. *Nano Lett.* **15**, 8148–8154 (2015).

(44) Buckman, J.F. et al. MitoTracker labeling in primary neuronal and astrocytic cultures: influence of mitochondrial membrane potential and oxidants. *J Neurosci Methods* **104**, 165–76 (2001).

Acknowledgements

This work was partly supported instrumentally by Moscow State University Program of Development. NAB acknowledges support from Russian Foundation for Basic Research (RFBR, grant number 20-04-01011a), AAS acknowledges support from Russian Science Foundation (RSF, grant number 20-73-00257). AVA and SMN acknowledge support from Russian Foundation for Basic Research (RFBR, grants number 20-07-00840a and 20-07-00475a). GVM acknowledges support from Russian Science Foundation (RSF, grant number 19-79-30062). We are grateful to Olga Eremina for the assistance in AgNSS preparation and to Alexey Brazhe for the help with SERS and Raman spectra analysis. We are thankful to Ib Therkelsen Arent for the assistance in mitochondria preparation.

Author information

Contributions

N.A.B, E.I.N.,G.V.M., E.A.G., O.S. and A.B.R. conceived the experiments. N.A.B., E.I.N., SMN and O.S. performed SERS experiments and analysed SERS spectra; A.A.S. and E.A.G. designed AgNSSs; A.A.S., E.A.G. and E.I.N. fabricated AgNSSs. N.A.B., E.I.N., Z.V.B. and A.A.B. prepared mitochondria samples; E.I.N. and V.G.G prepared liposomes with cytC; V.G.G. prepared inverted mitochondria; E.I.N., Z.V.B. and A.A.B. performed respirometry experiments and their analysis. A.A.S. and E.A.G. performed the electron microscopy (SEM) analysis. S.M.N. conducted optical spectroscopy. V.S.V., D.I.Y. A.B.E. and A.V.A. performed SNOM characterization. N.A.B., G.V.M., E.A.G., O.S. and A.B.R. contributed tools and materials. A.B.R. and O.S. supervised the project. N.A.B., E.I.N., S.M.N. and O.S. drafted the manuscript. All authors discussed the results, edited and commented on the manuscript.

Corresponding authors

Correspondence to Nadezda A. Brazhe and Olga Sosnovtseva

Ethics declarations

Competing interests

The authors declare no competing financial interests

Supplementary information

Supplementary Figures 1-10, Supplementary Table 1